

# Loss of $\alpha 10\beta 1$ integrin expression leads to moderate dysfunction of growth plate chondrocytes

Therese Bengtsson<sup>1,2</sup>, Attila Aszodi<sup>3</sup>, Claudia Nicolae<sup>3</sup>, Ernst B. Hunziker<sup>4</sup>, Evy Lundgren-Åkerlund<sup>2</sup> and Reinhard Fässler<sup>1,3,\*</sup>

<sup>1</sup>Department of Experimental Pathology, Lund University Hospital, Box 117, 22185 Lund, Sweden

<sup>2</sup>Cartela AB, BioMedical Center I12, Sölvegatan 19, 22184 Lund, Sweden

<sup>3</sup>Max Planck Institute of Biochemistry, Department for Molecular Medicine, Am Klopferspitz 18, 82152 Martinsried, Germany

<sup>4</sup>ITI Research Institute for Dental and Skeletal Biology, University of Bern, Murtenstrasse 35, PO Box 54, CH- 3010 Bern, Switzerland

\*Author for correspondence (e-mail: faessler@biochem.mpg.de)

Accepted 8 December 2004

Journal of Cell Science 118, 929-936 Published by The Company of Biologists 2005

doi:10.1242/jcs.01678

## Summary

Integrin  $\alpha 10\beta 1$  is a collagen-binding integrin expressed on chondrocytes. In order to unravel the role of the  $\alpha 10$  integrin during development, we generated mice carrying a constitutive deletion of the  $\alpha 10$  integrin gene. The mutant mice had a normal lifespan and were fertile but developed a growth retardation of the long bones. Analysis of the skeleton revealed defects in the growth plate after birth characterized by a disturbed columnar arrangement of chondrocytes, abnormal chondrocyte shape and reduced

chondrocyte proliferation. Electron microscopy of growth plates from newborn mice revealed an increased number of apoptotic chondrocytes and reduced density of the collagen fibrillar network compared to these structures in control mice. These results demonstrate that integrin  $\alpha 10\beta 1$  plays a specific role in growth plate morphogenesis and function.

Key words: Integrin, Knockout, Cartilage, Growth plate, Proliferation

## Introduction

The major part of the mammalian skeleton forms via cartilaginous intermediates in a process called endochondral ossification (EO) (Aszodi et al., 2000). EO starts with the condensation of mesenchymal cells and their subsequent transformation into rounded chondrocytes leading to the formation of a cartilage mould already resembling the shape of future bones. The cartilaginous mould is surrounded by cells that lay down the perichondrium, a dense connective tissue, which separates cartilage from adjacent tissues. In long bones, a specialized structure called the growth plate is responsible for the linear growth and forms just below the epiphysis at both ends of the cartilaginous mould. Growth plate chondrocytes are organized into columns longitudinally and into zones horizontally. The zones reflect the sequential differentiation stages of chondrocyte proliferation, maturation and hypertrophy. In the proliferative zone, the chondrocytes assume a flattened appearance, are organized into stacks and actively divide. Later, the chondrocytes mature, become post-mitotic and slightly increase in size forming a narrow transition zone (called the maturation or prehypertrophic zone) between the proliferative and hypertrophic zones. In the hypertrophic zone, the cells become spherical and greatly enlarged. In the terminal area of the hypertrophic zone, the chondrocytes undergo apoptosis, vasculature invades the mineralized matrix and the cartilage is replaced by bone (primary ossification). During postnatal development, a second ossification process occurs at the epiphyseal parts of the growing bones and only articular cartilage remains at both ends.

The morphogenetic events of EO are accompanied by changes of the composition of the extracellular matrix (ECM).

The initial mesenchymal matrix contains evenly distributed collagen types I and III, and fibronectin. Transformation into hyaline cartilage is accompanied with the formation of a meshwork of collagen fibrils containing collagens II, IX and XI, which entrap aggregates of proteoglycans such as aggrecan and various adaptor and modulator proteins. Specialized cartilage, such as the hypertrophic cartilage in growth plates, contain collagen X. Bone matrix is characterized by the massive deposition of type I collagen.

Cartilage development and function crucially depends on the interaction of chondrocytes with the surrounding ECM. These interactions are primarily mediated by members of the integrin family of cell surface receptors. Integrins are  $\alpha\beta$  heterodimers, which link the ECM with the actin cytoskeleton and various signalling pathways that modulate differentiation, proliferation, survival and matrix assembly (Brakebusch et al., 2002; Hynes, 2002). Chondrocytes, depending on the species and tissue location, express a characteristic set of integrins including receptors for collagen type II ( $\alpha 1\beta 1$ ,  $\alpha 2\beta 1$  and  $\alpha 10\beta 1$ ), fibronectin ( $\alpha 5\beta 1$ ,  $\alpha v\beta 3$ ,  $\alpha v\beta 5$ ) and laminin ( $\alpha 6\beta 1$ ) (Camper et al., 1998; Loeser, 2000). In mice, the collagen-binding integrins display a differential expression pattern in developing cartilage. Immunohistochemistry revealed that  $\alpha 10\beta 1$  is expressed on epiphyseal as well as growth plate chondrocytes,  $\alpha 1\beta 1$  is highly expressed on articular chondrocytes and at lower levels on epiphyseal and growth plate chondrocytes, whereas  $\alpha 2\beta 1$  is not detected on mouse chondrocytes (Camper et al., 2001). These observations suggest that  $\alpha 10\beta 1$  is the major integrin mediating chondrocyte-collagen interactions in cartilage. In addition to cartilage,  $\alpha 10\beta 1$  antibodies stain the perichondrium, the valves

of the heart, the fascia of skeletal muscle and the surface of ligaments (Camper et al., 2001).

The importance of  $\beta 1$  integrin-mediated cell-matrix interactions during EO was recently addressed in our laboratory. Mice carrying a cartilage-specific deletion of the  $\beta 1$  integrin gene display a severe chondrodysplasia characterized by the complete lack of chondrocyte columns in growth plates, distorted collagen fibrillar network in the cartilage matrix and decreased proliferation of chondrocytes caused by abnormal G1/S transition and cytokinesis (Aszodi et al., 2003). As mice lacking other integrin subunits expressed on chondrocytes such as  $\alpha 1$ ,  $\alpha 2$ ,  $\alpha 6$ ,  $\alpha v$ ,  $\beta 3$  and  $\beta 5$  do not show an overt skeletal phenotype (Bouvard et al., 2001), the severe defects of the  $\beta 1$  integrin-null cartilage can be explained either by the simultaneous ablation of several  $\beta 1$  subunit containing integrins or by the loss of integrin  $\alpha 10\beta 1$ . To distinguish between these two possibilities, we generated mice lacking the  $\alpha 10$  integrin gene. We show that  $\alpha 10$ -null mice are viable and display a mild chondrodysplasia characterized by a mild disorganization of the growth plate and reduced proliferation of chondrocytes. These results indicate that the integrin  $\alpha 10\beta 1$  is important but not essential for endochondral ossification and that other collagen-binding integrins such as  $\alpha 2\beta 1$  compensate for its loss.

## Materials and Methods

### Generation of $\alpha 10$ integrin-deficient mice

Overlapping genomic clones covering the mouse  $\alpha 10$  integrin gene were isolated from a 129/Sv library as described (Bengtsson et al., 2001). The  $\alpha 10$  integrin gene was disrupted by inserting a cassette containing the enhanced green fluorescent protein (EGFP) gene and a loxP flanked neomycin gene (NEO) into exon 1. The construct was linearized with *NorI* and electroporated into R1 embryonic stem (ES) cells following standard protocols (Fässler and Meyer, 1995). Following G418 selection, targeted ES cell clones were identified by Southern blotting of *XbaI*-digested DNA. Two correctly targeted ES cell clones were injected into C57BL/6 blastocysts and male chimeras were subsequently mated with C57BL/6 females to establish  $\alpha 10$ -deficient mouse strains.

### Analysis of the skeleton

To visualize the whole skeleton, Alcian Blue/Alizarin Red staining of newborn, 8-week and 12-week-old mice and X-ray analysis of 4-week, 8-week, 12-week and 1-year-old mice were performed as described (Aszodi et al., 1998). At each stage, at least five wild type and five mutant animals were analyzed for the length of the various skeletal elements. For histological analysis, specimens (newborn, 2 weeks, 4 weeks, 8 weeks and 12 weeks old) were fixed overnight in 4% paraformaldehyde (PFA) in phosphate-buffered saline, pH 7.4 (PBS). Samples taken after birth were decalcified in 10% EDTA/PBS for 1-2 weeks. After embedding in paraffin, sections of 6-8  $\mu$ m were cut and stained with Hematoxylin and Eosin (HE). For morphometric analysis of the growth plate zones, tibiae from newborn, 2-week, and 4-week-old wild-type and mutant mice were processed (five animals per genotype and age group) and at least three sections from each sample were investigated by light microscopy as described earlier (Aszodi et al., 2003). At the newborn stage, two morphologically distinct zones (proliferative and hypertrophic) were measured in three locations of each section. The proliferative zone was defined as an area represented by flattened, stack-forming chondrocytes. The hypertrophic zone was defined by rounded and enlarged chondrocytes. The length of the narrow transition (prehypertrophic or maturation)

zone between the proliferative and hypertrophic zones was measured as part of the proliferative zone. At 2 weeks and 4 weeks of age, the length of the resting zone between the secondary ossification centre and the proliferation zone was also measured. The resting zone was defined by small, spherical chondrocytes separated by an abundant ECM. Apoptotic and proliferative chondrocytes were detected with the in situ cell death detection kit (Roche Diagnostics) and the BrdU (5-bromo-2'-deoxyuridine) incorporation assay (Aszodi et al., 1998), respectively. Cell death was further analyzed by electron microscopy according to morphological criteria described (Patwari et al., 2004). Immunostaining and ultrastructural analysis were carried out as previously described (Aszodi et al., 1998). Antibodies for immunohistochemistry were detailed earlier (Camper et al., 1998, Aszodi et al., 1998). The statistical analyses were performed according to standard procedures and statistical evaluation was done using *t*-test analysis. A value of  $P < 0.05$  was considered significant.

### RNA isolation, RT-PCR and in situ hybridization

Total RNA from hearts of 4-week-old wild-type, heterozygous and homozygous mutant mice was isolated using the RNeasy Kit (Qiagen). For reverse transcription (RT), 3.7  $\mu$ g total RNA was transcribed into cDNA using the Superscript<sup>TM</sup> II RNase H-Reverse Transcriptase synthesis system (Life Technologies). Aliquots of the reverse-transcribed material were amplified by PCR using primers specific for the  $\alpha 10$  integrin coding sequences (exon-1 specific forward primer, 5'-TGGAGTCTCTCCATCC-3' and exon 6-specific reverse primer, 5'-TCGATGAACAGTCTTCTACCAGC-3'). As a positive control,  $\beta$ -actin-specific primers (forward, 5'-GTGGGCCGCTCTAGGCACCAA-3' and reverse, 5'-CTCTTTGATGTCACGCACGATTTC-3') were used. In situ hybridization for cartilage differentiation markers was performed as described previously (Aszodi et al., 2003).

### Assays with primary chondrocytes

Chondrocytes from rib or limb cartilage were released by using a collagenase type II (Worthington) digestion protocol as described (Bengtsson et al., 2001). Adhesion assays were performed with primary wild type and mutant chondrocytes on 48-well plates coated with collagen types I, II, fibronectin or BSA (10  $\mu$ g/ml each) as described (Camper et al., 1997). For cell spreading, primary chondrocytes were seeded in DMEM supplemented with 0.5% FCS on eight-well glass Lab-Tek chamber slides (Nalge Nunc International) coated with collagen type II or fibronectin. Cells were allowed to spread for 3 days then subjected to antibody staining. For flow cytometry, primary chondrocytes were incubated with hamster monoclonal antibodies (mAb) against the integrin subunits  $\alpha 1$ ,  $\alpha 2$  and  $\beta 1$  (all obtained from Pharmingen), with a rat mAb against  $\alpha 5$  integrin (Pharmingen), with a mouse mAb against  $\alpha 10$  or a mouse antisera against the  $\alpha 11$  integrin (E.L.-A., unpublished) for 20 minutes on ice. After washing, cells were incubated with the appropriate phycoerythrin-conjugated secondary antibody (Becton Dickinson) and analyzed for fluorescence with a FACSCAN flow cytometer (Becton Dickinson).

To detect the  $\alpha 10$  integrin protein on chondrocytes, primary rib chondrocytes were cell surface biotinylated, lysed and immunoprecipitated with antisera raised against the  $\alpha 10$  integrin and analyzed by western blotting as described (Bengtsson et al., 2001).

## Results

### Generation of $\alpha 10$ integrin-deficient mice

To ablate the  $\alpha 10$  integrin gene in ES cells an *EGFP-loxP-neo-loxP* cassette was used to replace the entire exon 1. This results in the disruption of the open reading frame immediately after

the translation initiation codon (Fig. 1A). Two targeted ES cell clones were used to generate germline chimeric mice (Fig. 1B). RT-PCR analysis of total RNA isolated from heart lacked  $\alpha 10$  integrin mRNA in homozygous mutant mice (Fig. 1C). Loss of the  $\alpha 10$  integrin protein in  $\alpha 10^{-/-}$  mice was demonstrated by immunostaining of newborn knee cartilage (Fig. 1D) and by western blotting of chondrocyte lysates (data not shown). Southern blot analysis of 242 offspring from heterozygous intercrosses revealed normal Mendelian transmission of the mutant  $\alpha 10$  integrin gene (data not shown). Homozygous mutant mice were fertile and had a normal life span.

### $\alpha 10$ integrin-deficient mice display moderate shortening of long bones and growth plate defects

As  $\alpha 10$  integrin is mainly expressed in cartilage (Camper et al., 2001) the skeleton was analyzed at various developmental

stages. For gross inspection, whole mount skeletons of newborn, 8-week, 12-week and 1-year-old mutant and wild-type mice were analyzed by Alcian Blue/Alizarin Red staining (Fig. 2A,B) or X-ray irradiation (Fig. 2C). These investigations revealed that all skeletal elements of mutant mice looked normal, however, the length of the long bones was slightly reduced in mutants compared to control animals (Fig. 2D). At birth and 8 weeks of age the length reduction of tibia and femur was very moderate (2-3% from controls) and statistically not significant. At later stages the difference increased to 7-10% and became statistically significant ( $P < 0.05$ , five animals/genotype).

Next, we analyzed the structure of the cartilage at light and electron microscopic (EM) level. At birth, Hematoxylin-Eosin staining of serial sections of wild-type and mutant tibiae showed a clear separation of epiphyseal and growth plate cartilage (Fig. 3A). The morphological appearance of the epiphyseal cartilage was indistinguishable but the mutant growth plates showed several mild abnormalities when compared to controls. First, the  $\alpha 10$ -null growth plate was still organized into distinct zones of proliferative, prehypertrophic and hypertrophic chondrocytes. The length of the hypertrophic zone, however, was moderately shortened compared to the wild type (Fig. 3A,E). In the wild type, the hypertrophic zone consisted of 4-5 cell layers, whereas in the mutant it consisted of only 2-3 cell layers (Fig. 3A). Morphometric measurements revealed that the lengths of the control and mutant hypertrophic zone were  $237 \pm 12 \mu\text{m}$  and  $180 \pm 14 \mu\text{m}$ , respectively ( $P < 0.0001$ ) (Fig. 3E). The length of the proliferative/prehypertrophic zones was  $474 \pm 44 \mu\text{m}$  in the wild type and  $471 \pm 49 \mu\text{m}$  in the mutant, and showed no statistically significant difference (Fig. 3A,E). Second, histological and EM analyses showed that in the proliferative zone  $\alpha 10$ -null chondrocytes were more rounded compared to the normal, flattened shape of control chondrocytes, and failed to organize into well-formed columns in most of the mutant growth plates (Fig. 3A,B). The disturbance of the columnar structure was more prominent at the central part of the growth plate, and was less obvious at the regions adjacent to the perichondrium/periosteum (Fig. 3A). In addition, EM of two wild-type and two mutant cartilage samples revealed the presence of few apoptotic chondrocytes (less than one percent of the chondrocytes analyzed), scattered throughout the mutant proliferative and hypertrophic zone (Fig. 3C and data not shown). The most frequently observed morphological features for apoptotic chondrocytes (Patwari et al., 2004) in the mutant growth plate were chondrocyte shrinkage, condensation of the chromatin, intense staining of the cytoplasm and nuclear blebbing. To further confirm these ultrastructural findings, cell death was analyzed using a TUNEL (terminal deoxynucleotidyl transferase mediated dUTP nick and labeling) assay on newborn tibial sections. In the wild type, apoptosis was detectable in cells at the chondro-osseous junction and the perichondrium/periosteum but was never observed in chondrocytes of the growth plate or epiphyseal cartilage (Fig. 3C). In contrast, apoptotic chondrocytes were clearly detectable in the proliferative/prehypertrophic and the hypertrophic zones of the mutant growth plate (Fig. 3C). However, the number of TUNEL-positive chondrocytes was low. We found on average three to four apoptotic cells per six sections representing various areas of the tibial cartilage. This

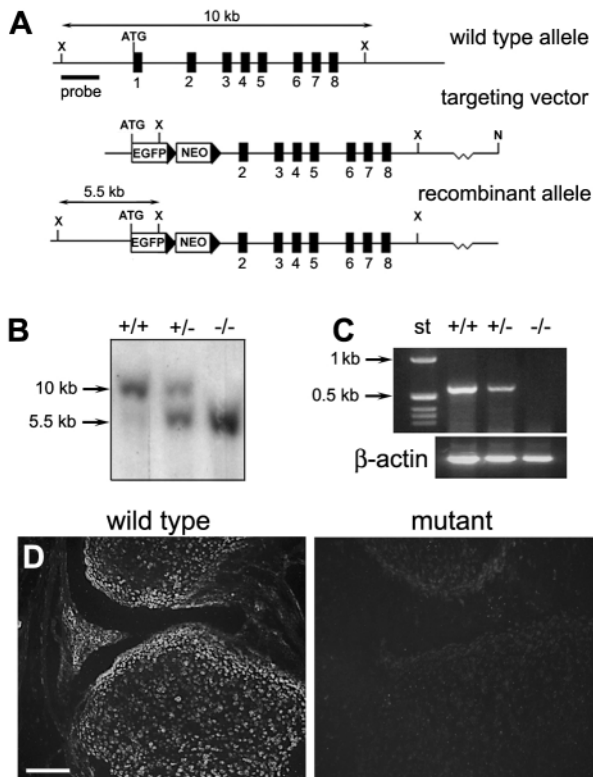


**Fig. 1.** Generation of  $\alpha 10$  integrin-null mice. (A) Organization of the mouse  $\alpha 10$  integrin gene, targeting construct and recombinant allele. Exons are numbered and indicated by black boxes. EGFP, enhanced green fluorescent protein; NEO, neomycin resistance gene. Relevant restriction sites: X, *Xba*I; N, *Nor*I. Probe denotes the external probe used for Southern genotyping, which detects (B) Southern blot analysis of mouse tail DNA derived from progeny of heterozygous breeding (+/+, wild-type; +/-, heterozygous; -/- homozygous mutant). The  $\alpha 10$  integrin probe indicated in A detects a 10 kb fragment and a 5.5 kb fragment in the wild type and knockout alleles, respectively. (C) RT-PCR analysis of mRNA isolated from the heart indicates a complete lack of the  $\alpha 10$  integrin transcript in homozygous mutant (-/-) mice. st, molecular weight standards. (D) Immunohistochemical staining of the knee region from newborn wild-type and mutant mice using an  $\alpha 10$  integrin-specific polyclonal antibody. Mutant chondrocytes show negative staining for  $\alpha 10$  integrin. Bar, 100  $\mu\text{m}$ .

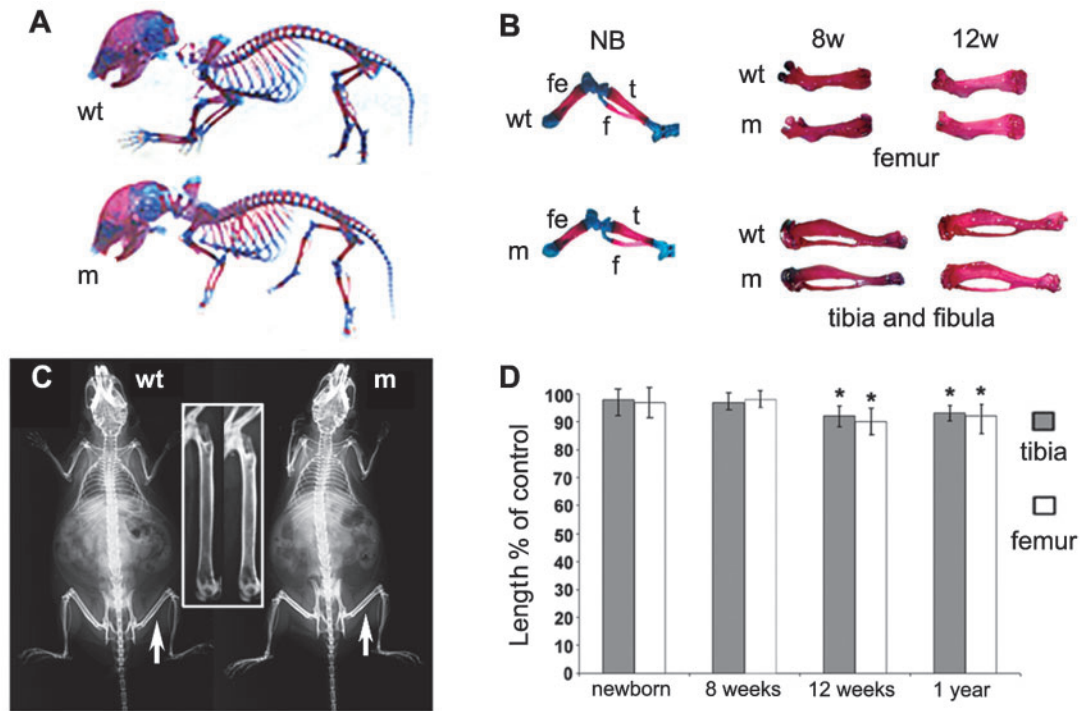


**Fig. 2.** Skeletal analysis of  $\alpha 10$ -deficient mice. (A) Staining with Alcian Blue and Alizarin Red shows no obvious skeletal defect of mutant (m) mice compared to wild-type (wt) mice at the newborn stage. (B) Skeletal staining of hindlimbs of newborn (NB), 8-week-old (8w) and 12-week-old (12w) animals. (C) X-ray analysis of 1-year-old mice indicates a slight, time progressive shortening of the long bones. The insets in C show magnified images of the wild-type and mutant femur (arrows). (D) Diagram showing the relative length of the tibia and femur of  $\alpha 10$  integrin-null mice compared to the wild type at various ages. Bars represent mean  $\pm$  s.d. A significant difference in bone length was measured in mutants compared to that in control mice \* $P < 0.05$ ,  $n = 5$  animals per genotype.

apoptotic rate was at a similarly low rate as observed in the  $\beta 1$  integrin-deficient cartilage (Aszodi et al., 2003).

During postnatal development (2 weeks, 4 weeks and 8 weeks of age), the mild shape change of the proliferative chondrocytes and the slight disorganization of the columnar structure were frequently observed in mutant growth plates (Fig. 3D and data not shown). The reduced hypertrophic zone was also characteristic for the mutant (Fig. 3D,E). At 2 weeks of age, the length of the wild type hypertrophic zone was  $205 \pm 29 \mu\text{m}$ , whereas the length of the mutant hypertrophic zone was  $147 \pm 12 \mu\text{m}$  ( $P < 0.0001$ ) (Fig. 3E). At 4 weeks, the lengths of the hypertrophic zone were  $171 \pm 11 \mu\text{m}$  in the wild type and  $136 \pm 7 \mu\text{m}$  in the mutant ( $P < 0.0001$ ) (Fig. 3E). The lengths of the mutant resting and the proliferative zones were not statistically different to the lengths of these zones in wild-type mice (Fig. 3E).

To analyse the consequence of the lack of  $\alpha 10$  integrin on endochondral bone formation further, we performed analysis of chondrocyte differentiation at the newborn stage. Using in situ hybridization, the expression of type II collagen (*Col2a1*, a marker for non-hypertrophic chondrocytes), Indian hedgehog (*Ihh*) and parathyroid hormone/parathyroid-hormone-related-peptide receptor (*PP-R*) (markers for prehypertrophic zone) was found to be normal in the mutant mice (Fig. 4A,C,D). Collagen X mRNA (*Col10a1*) was found in the hypertrophic and the lower prehypertrophic zones of the growth plate of both control and mutant mice but the collagen X expression domain was slightly reduced in the mutant compared to the wild type

(Fig. 4B). This finding is in agreement with the histological observation indicating a shorter hypertrophic zone in the mutant (Fig. 3A). Finally, by histochemical staining for osteoblasts (alkaline phosphatase) and osteoclasts (tartrate-resistant acid-phosphatase) we could not detect a difference between wild type and mutant animals (data not shown).

In addition to the cellular and columnar abnormalities, EM revealed an altered cartilage matrix in mutant growth plates. The density of the collagen fibrillar network was slightly reduced in all (pericellular, territorial and interterritorial) matrix compartments (Fig. 5A,B) of the proliferative zone, but the mesh-like organization of the collagen fibrils appeared normal in the mutant. By immunohistochemistry we could not detect a difference in the deposition of cartilage matrix proteins such as collagen II, matrilin-1, matrilin-3, and aggrecan (Fig. 5C and data not shown). However, the deposition of collagen X in the mutant growth plate was not restricted to the hypertrophic/prehypertrophic zones as in the wild type but extended deeper into the proliferative zone (Fig. 5D). The apparent discrepancy between the reduced collagen X mRNA expression and the expanded protein deposition patterns in the mutant could result from the reduced fibrillar collagen network in the mutant cartilage matrix leading to diffusion of collagen X into the proliferative zone.

#### Impaired proliferation of $\alpha 10$ -deficient chondrocytes

The growth of long bones depends on chondrocyte

proliferation. Therefore, we compared the proliferation rates in wild-type and mutant growth plates at various stages of development. The labeling index of chondrocytes in the S phase of the cell cycle, demonstrated by BrdU (5-bromo-2'-deoxyuridine) incorporation, was significantly lower in mutant growth plates when compared with the wild type both at birth and at 2 weeks of age (Fig. 6A; 35% and 21% reduction, respectively,  $n=8-12$ ). At later stages (4 and 8 weeks), the reduction of the proliferation rate was less pronounced (Fig. 6A and data not shown). Immunostaining for cyclin-D, a marker for G1 phase progression, led to a similar result (Fig.

6B) showing a mild, but statistically significant decrease of cyclin-D-positive nuclei in  $\alpha 10$ -deficient growth plates in newborn, 2 weeks and 4 weeks of age ( $n=3$ ; five sections/animal). The G1/S transition defect was accompanied with the increased nuclear translocation of Stat1 and Stat5a, members of the family of signal transducers and activators of transcription, and increased production of the cell cycle inhibitor p16 in the proliferative zone of the mutant growth plates (Fig. 6C,  $n=3$ ; five consecutive sections/animal). In  $\beta 1$ -deficient chondrocytes elevated nuclear translocation of Stat proteins and upregulation of p16 were associated with increased levels of the fibroblast growth factor receptor 3 (*Fgfr3*) transcript (Aszodi et al., 2003). Therefore, we investigated *Fgfr3* expression in  $\alpha 10$  mutants. In situ hybridization at E15.5, however, revealed no detectable difference in *Fgfr3* expression in growth plates (Fig. 6D).

### Mutant chondrocytes show normal adhesion to collagens in vitro

As  $\alpha 10\beta 1$  is proposed to be the major collagen-binding integrin in cartilage, we studied the adhesive properties of  $\alpha 10$ -deficient chondrocytes to fibrillar collagens. Surprisingly, the adhesion of  $\alpha 10$ -integrin-deficient primary chondrocytes to collagen type I and type II was not reduced when compared to the wild type (Fig. 7A). Similarly, the adhesion to fibronectin was not different between mutant and control chondrocytes (Fig. 7A). To analyse if chondrocyte spreading was affected in the absence of the  $\alpha 10\beta 1$  integrin, we performed spreading assays on various substrates. Mutant as well as wild-type

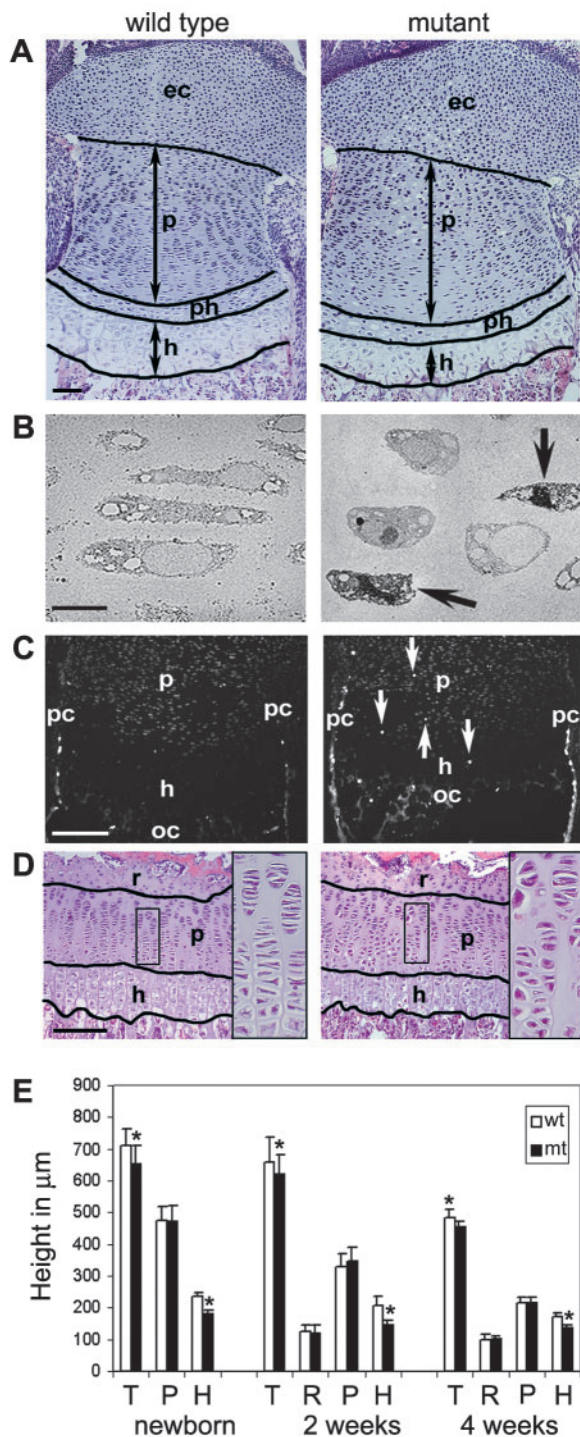


**Fig. 3.** Analysis of cartilage development. (A) Hematoxylin/Eosin-stained sections through the tibia of newborn mice. The epiphyseal cartilage (ec) and the length of the proliferative (p) and prehypertrophic (ph) zones are apparently normal, but the length of the hypertrophic zone (h) is reduced in the  $\alpha 10$  integrin-deficient growth plate. In the proliferative zone, the wild type chondrocytes are flattened and show a typical stack-like arrangement. In the mutant growth plate, the proliferative chondrocytes are more rounded, and their stack-like organization is slightly impaired. (B) Electron micrographs of clusters of proliferative cells at the newborn stage. Arrows indicate degenerative cells characterized by cell shrinkage, chromatin condensation and intense cytoplasmic staining in the mutant growth plate. Note, the round shape of the mutant chondrocytes compared to the flattened shape of the control chondrocytes. (C) TUNEL assay at the newborn stage demonstrates apoptotic chondrocytes (arrows) in the proliferative (p) and hypertrophic (h) zones of the mutant growth plate but not in the control growth plate. Apoptotic chondrocytes were detectable at the perichondrium (pc) and osseochondrogenic junction (oc) in both the wild type and mutant. (D) Hematoxylin/Eosin-stained tibiae at 2 weeks of age. In the mutant growth plate, the columns are less organized and the chondrocytes are more rounded (compare also insets). The length of the hypertrophic zone (h) is reduced in the mutant compared to the wild type. r, resting zone. (E) Morphometric analysis demonstrating the lengths of the total growth plate (T), proliferative/prehypertrophic zone (P), hypertrophic zone (H) and the resting zone (R, at 2 weeks and 4 weeks) in wild-type (wt) and mutant (mt) mice at various ages. The lengths of the total growth plate and the hypertrophic zone were slightly, but significantly reduced in the mutant at each age group when compared to lengths at appropriate stages of the control mice ( $*P<0.0001$ ). Results represent mean $\pm$ s.d. of five animals per genotype and age group with three sections analyzed per animal. Bar, 100  $\mu\text{m}$  (A,C,D); 50 nm (B).

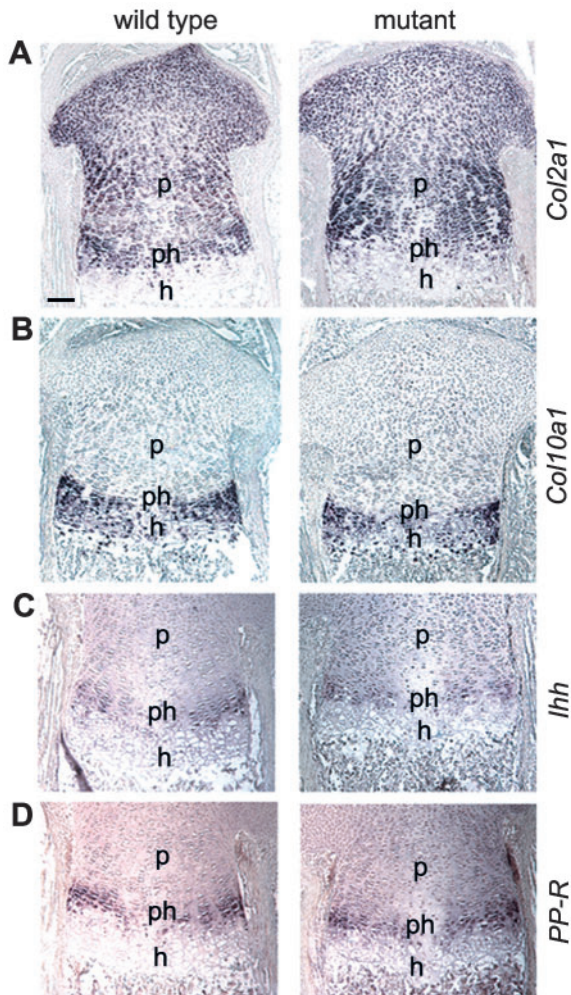


**Fig. 4.** In situ hybridization analysis for cartilage differentiation. Newborn tibial sections were hybridized with riboprobes specific for (A) collagen II (*Col2a1*, a marker for non-hypertrophic chondrocytes), (B) collagen X (*Col10a1*, a marker for hypertrophic and distal prehypertrophic chondrocytes), (C) Indian hedgehog (*Ihh*) and (D) PTH/PTHrP receptor (*PP-R*) (markers for prehypertrophic chondrocytes). In the mutant the expression domain of *Col10a1* was slightly reduced compared to that in the wild type, whereas the other markers were expressed normally. ec, epiphyseal cartilage; h, hypertrophic zone; p, proliferative zone; ph, prehypertrophic zone. Bar, 100  $\mu$ m.

chondrocytes remained round when adhered to collagen types I and II, whereas both control and  $\alpha 10$ -deficient cells spread normally on fibronectin and vitronectin (data not shown). Immunostaining with phalloidin and for vinculin indicated normal cytoskeletal organization and focal contact formation in mutant chondrocytes (data not shown).

One possible explanation for the normal adhesion of the  $\alpha 10$  null chondrocytes on collagens could be that other collagen-binding integrins compensate for the loss of  $\alpha 10\beta 1$ . To test their expression levels we performed FACS analysis using specific antibodies against the  $\beta 1$  and various  $\alpha$  subunits (Fig. 7B). Mutant primary chondrocytes from limb cartilage showed no expression of the  $\alpha 10$  subunit and a reduced expression of the  $\beta 1$  integrin compared to the wild type. The collagen-

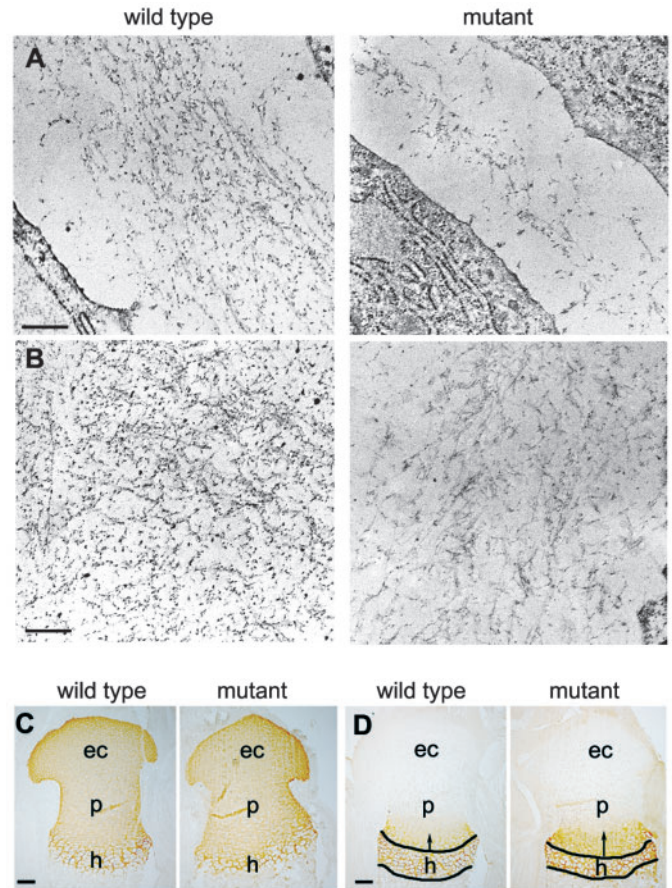


**Fig. 5.** Analysis of the collagen matrix in wild-type and mutant cartilage. (A,B) Electron micrographs of the pericellular and territorial (A) and the interterritorial (B) matrix compartments of wild-type and mutant growth plates at the newborn stage. Note the reduced collagen fibril density in the mutant compared to that in the wild type. (C,D) Immunohistochemical staining of the tibia for collagen type II (Col2) and type X (Col10) at the newborn stage. Collagen X was deposited in the hypertrophic (h) zone in both control and mutant mice. Note that the hypertrophic zone is smaller and that the collagen X staining extends deeper into the prehypertrophic/proliferative (p) zone in mutant cartilage. ec, epiphyseal cartilage. Bar, 400 nm (A and B); 100  $\mu$ m (C and D).

binding  $\alpha 2\beta 1$  and  $\alpha 11\beta 1$  integrins were undetectable both on control and mutant chondrocytes. However, we could observe a significant, comparable expression level of the  $\alpha 1$  subunit on both  $\alpha 10$ -deficient and wild-type chondrocytes suggesting that  $\alpha 1\beta 1$  might compensate the loss of  $\alpha 10\beta 1$ .

## Discussion

Proper development and function of tissues strongly depend on cell-matrix interactions, which are mediated mainly by integrins. Cartilage is unique among the tissues because each chondrocyte is surrounded by a specialized matrix, which contains vast amounts of collagen as the primary adhesive protein. It has been reported that chondrocytes of various species express several collagen-binding integrins including integrins  $\alpha 1\beta 1$ ,  $\alpha 2\beta 1$  and the recently identified  $\alpha 10\beta 1$ . In this paper, we describe the targeted inactivation of the mouse  $\alpha 10$

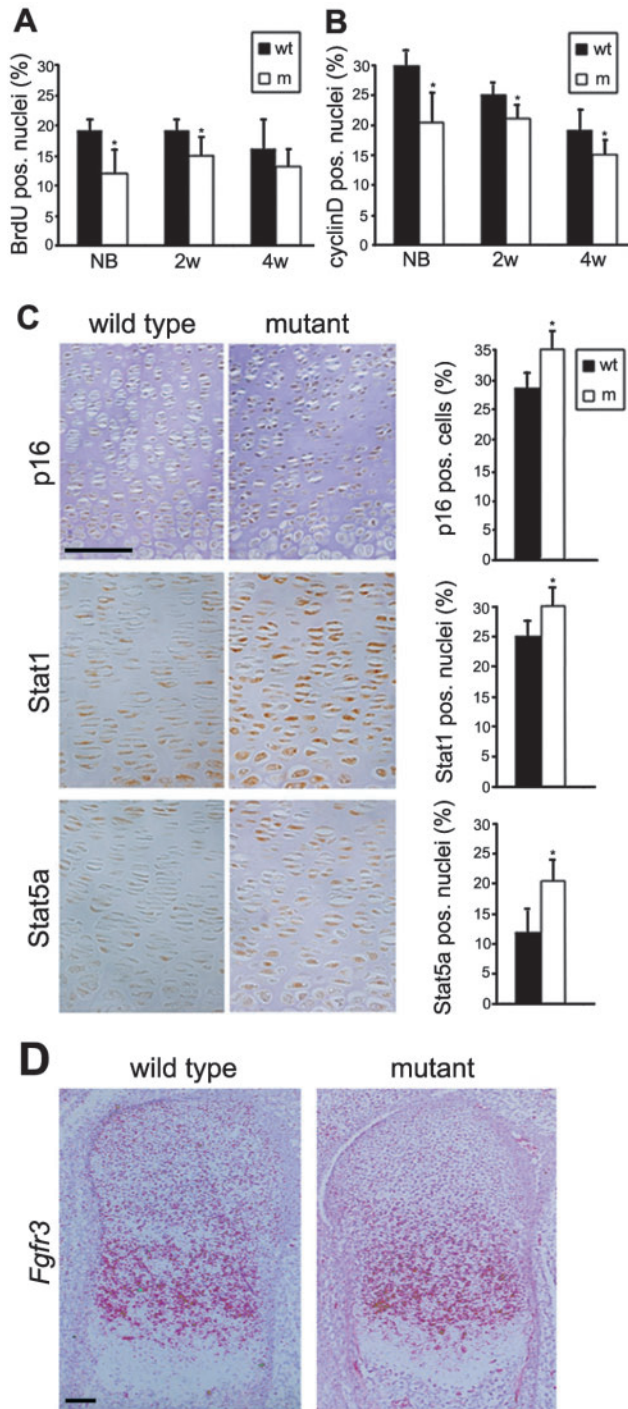


**Fig. 6.** Defective G1 progression in  $\alpha 10$ -null proliferative chondrocytes. Reduction of BrdU-labelled (A) and cyclin-D-positive (B) nuclei of mutant proliferative chondrocytes in newborn (NB) mice and in mice at 2 weeks (2w) and 4 weeks (4w) of age. Bars represent mean  $\pm$  s.d. \* $P < 0.05$  compared to numbers in relevant control mice. Five sections from eight to twelve animals (A) and three animals (B) were analyzed per genotype. (C) Immunohistochemistry at the newborn stage reveals elevated expression of p16 and increased nuclear translocation of Stat1 and Stat5a in the proliferative zone of mutant growth plates compared to that in the wild type ( $n = 3$  animals per genotype and  $n = 5$  sections per animal). (D) In situ hybridization shows comparable expression levels of *Fgfr3* in femurs from wild-type and mutant mice at E15.5. Bar, 100  $\mu$ m.

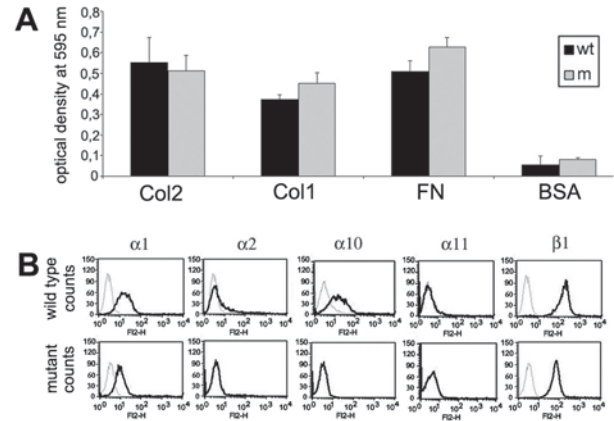


**Fig. 7.** Assays with primary chondrocytes. (A) Normal adhesion of mutant chondrocytes to collagen type II (Col2), collagen type I (Col1), fibronectin (FN) and bovine serum albumin (BSA). The y-axis shows the adherent cells as a percentage of the total number added per well. Shown are the mean  $\pm$  s.d. of experiments carried out in triplicate. (B) FACS analysis of integrin expression on primary chondrocytes isolated from newborn limb cartilage.

integrin gene and demonstrate for the first time the involvement of an  $\alpha$  subunit in endochondral bone formation. Integrin  $\alpha 10$ -deficient mice develop a mild chondrodysplasia characterized by chondrocyte shape change, reduced proliferation rate, impaired columnar organization of the growth plate and decreased collagen fibril density in the cartilage matrix.

The biological role of integrin-mediated chondrocyte-matrix interactions was tested recently with a mouse strain carrying a cartilage-specific deletion of the  $\beta 1$  integrin gene (Aszodi et al., 2003). Mice lacking  $\beta 1$  integrins on chondrocytes develop severe skeletal abnormalities. In vitro,  $\beta 1$ -null chondrocytes are unable to adhere to collagen type II and laminin 1, display reduced binding to fibronectin and form fewer focal adhesions and stress fibres. The in vivo consequences of these defects are a rounder shape of the mutant proliferative chondrocytes and an inability to arrange into typical vertical columns within the growth plate. The lack of the columnar structure is due to the almost complete block of the rotational motility of the mutant chondrocytes, which is essential to form cell stacks parallel to the long axis of the developing bone (Doods, 1930). Mice lacking the laminin receptor  $\alpha 6\beta 1$  (Georges-Labouesse et al., 1996) as well as mice lacking fibronectin in cartilage (Aszodi et al., 2003) develop no obvious skeletal defects, and the structural disorganization of the  $\beta 1$ -null growth plate is probably caused by the loss of all collagen-binding  $\beta 1$  integrins ( $\alpha 1\beta 1$ ,  $\alpha 2\beta 1$  and  $\alpha 10\beta 1$ ) on chondrocytes. The importance of collagen-chondrocyte interaction is supported by the present study, which demonstrates the tendency of chondrocyte rounding and impaired stack-like organization of the proliferative chondrocytes in the  $\alpha 10$  integrin-deficient growth plates. However, these abnormalities are less severe when compared to the  $\beta 1$ -null growth plates indicating a partial redundancy among collagen-binding  $\beta 1$  integrins expressed on chondrocytes. The primary candidate for such a redundant collagen-binding integrin is  $\alpha 1\beta 1$ , which is expressed on freshly isolated mutant as well as control chondrocytes. Another remarkable similarity between  $\alpha 10$ - and  $\beta 1$ -deficient cartilages is the reduced collagen fibril density in many areas

of the mutant matrices. It has been shown earlier that the polymerization and deposition of fibronectin and laminin on the cell surface is modulated by  $\beta 1$  integrins (Wennerberg et al., 1996; Lohikangas et al., 2001). A recent study demonstrated that collagen deposition is also regulated by collagen-binding integrins in transfected mouse fibroblastic cell lines (Velling et al., 2002). In the presence of fibronectin, cells expressing integrins  $\alpha 2\beta 1$  or  $\alpha 11\beta 1$  were shown to deposit significantly more fibrillar collagen than cells lacking these integrins. Furthermore these cells, in the absence of fibronectin, were able to deposit collagens I and III, which never formed a typical network. These observations led to the concept that collagen matrix assembly is indirectly regulated through  $\alpha 5\beta 1$  integrin-mediated fibronectin deposition and enhanced directly via collagen-binding integrins (Velling et al., 2002). However, mice lacking the fibronectin gene in chondrocytes develop a normal skeleton (Aszodi et al., 2003) and the essential role of the pre-existing fibronectin pericellular matrix in collagen fibril assembly was not verified in cartilage in vivo. Therefore, the reduced fibrillar density in the matrices of  $\alpha 10$ - and  $\beta 1$ -deficient growth plates suggest that  $\beta 1$  integrins might directly modulate the polymerization of type II collagen fibrils and/or the incorporation of the fibrils into the collagen network. The impact of this reduced fibrillar density on cartilage development is not clear, but it could probably alter the diffusion properties of the matrix resulting in an extended deposition of the type X collagen into the maturation/proliferation zone of both the  $\alpha 10$ -null and the  $\beta 1$ -deficient growth plates (Aszodi et al., 2003) and a diffusion and dilution of growth factors.

Finally, both  $\alpha 10$ - and  $\beta 1$ -null chondrocytes (Aszodi et al., 2003) show impaired G1 progression of the cell cycle characterized by decreased BrdU incorporation and reduced cyclin D expression. However, these defects were again much milder in the  $\alpha 10$ -deficient mice. Chondrocyte proliferation is dependent on cell-matrix attachment and the concerted actions of various signaling molecules such as growth factors and morphogens (Karsenty and Wagner, 2002). Fibroblast growth factor (FGF) signaling via FGF receptor 3 (FGFR3) negatively regulates chondrocyte proliferation and its upregulation leads to dwarfing dysplasias in human (Ornitz and Marie, 2002). The underlying mechanism of the elevated FGF signaling is the nuclear translocation of Stat proteins and the subsequent upregulation of cell cycle inhibitors such as p16, p18, p19 and p21 (Ornitz and Marie, 2002). Analysis of  $\beta 1$ -deficient growth plates revealed increased expression of *Fgfr3*, increased levels of proteins p16 and p21, and increased nuclear translocation of Stat1/Stat5a demonstrating a cross talk between  $\beta 1$  integrins and FGFR3-mediated FGF signaling (Aszodi et al., 2003). Integrin  $\alpha 10$ -deficient chondrocytes display only a moderate increase in Stat1/Stat5a nuclear translocation and in the protein levels of p16; however, the expression level of *Fgfr3* did not change significantly compared to wild-type chondrocytes. This discrepancy raises two possibilities: either *Fgfr3* expression is only slightly elevated (escaping detection by in situ hybridization) or  $\alpha 10\beta 1$  modulates Stat translocation and p16 production by other, unknown signaling pathway(s).

Despite the described similarities,  $\alpha 10$ - and  $\beta 1$ -null chondrocytes exhibit marked differences. The  $\alpha 10$ -null cells show no gross abnormalities in organization of the actin

cytoskeleton and cytokinesis, which contribute to the severe alterations in the  $\beta 1$ -deficient growth plate (Aszodi et al., 2003), clearly indicating that the absence of multiple  $\beta 1$  subunit containing integrins on chondrocytes is required for the severe defects.

The authors thank Alison Pirro Lundqvist and Zsuzsanna Farkas for technical assistance. This work was supported by the Swedish Foundation for Strategic Research, Cartela AB, the Max Planck Society, the DFG and the Fonds der Chemischen Industrie.

## References

- Aszodi, A., Chan, D., Hunziker, E., Bateman, J. F. and Fässler, R. (1998). Collagen II is essential for the removal of the notochord and the formation of intervertebral discs. *J. Cell Biol.* **143**, 1399-1412.
- Aszodi, A., Bateman, J. F., Gustafsson, E., Boot-Handford, R. and Fässler, R. (2000). Mammalian skeletogenesis and extracellular matrix: what can we learn from knockout mice? *Cell Struct. Funct.* **25**, 73-84.
- Aszodi, A., Hunziker, E. B., Brakebusch, C. and Fässler, R. (2003). Beta1 integrins regulate chondrocyte rotation, G1 progression, and cytokinesis. *Genes Dev.* **17**, 2465-2479.
- Bengtsson, T., Camper, L., Schneller, M. and Lundgren-Åkerlund, E. (2001). Characterization of the mouse integrin subunit alpha10 gene and comparison with its human homologue. Genomic structure, chromosomal localization and identification of splice variants. *Matrix Biol.* **20**, 565-576.
- Bouvard, D., Brakebusch, C., Gustafsson, E., Aszodi, A., Bengtsson, T., Berna, A. and Fässler, R. (2001). Functional consequences of integrin gene mutations in mice. *Circ. Res.* **89**, 211-223.
- Brakebusch, C., Bouvard, D., Stanchi, F., Sakai, T. and Fässler, R. (2002). Integrins in invasive growth. *J. Clin. Invest.* **109**, 999-1006.
- Camper, L., Heinegard, D. and Lundgren-Åkerlund, E. (1997). Integrin alpha2beta1 is a receptor for the cartilage matrix protein chondroadherin. *J. Cell Biol.* **138**, 1159-1167.
- Camper, L., Hellman, U. and Lundgren-Åkerlund, E. (1998). Isolation, cloning, and sequence analysis of the integrin subunit alpha10, a beta1-associated collagen binding integrin expressed on chondrocytes. *J. Biol. Chem.* **273**, 20383-20389.
- Camper, L., Holmval, K., Wängnerud, C., Aszodi, A. and Lundgren-Åkerlund, E. (2001). Distribution of the collagen-binding integrin alpha10beta1 during mouse development. *Cell Tissue Res.* **306**, 107-116.
- Doods, G. S. (1930). Row formation and other types of arrangement of cartilage cells in endochondrial ossification. *Anat. Rec.* **46**, 385-399.
- Fässler, R. and Meyer, M. (1995). Consequences of lack of  $\beta 1$  integrin gene expression in mice. *Genes Dev.* **1**, 1896-1908.
- Georges-Labouesse, E., Messaddeq, N., Yehia, G., Cadalbert, L., Dierich, A. and Le Meur, M. (1996). Absence of integrin alpha 6 leads to epidermolysis bullosa and neonatal death in mice. *Nature Genet.* **13**, 370-373.
- Hynes, R. O. (2002). Integrins: bidirectional, allosteric signaling machines. *Cell.* **110**, 673-687.
- Karsenty, G. and Wagner, E. F. (2002). Reaching a genetic and molecular understanding of skeletal development. *Dev. Cell* **2**, 389-406.
- Loeser, R. F. (2000). Chondrocyte integrin expression and function. *Biorheology* **37**, 109-116.
- Lohikangas, L., Gullberg, D. and Johansson, S. (2001). Assembly of laminin polymers is dependent on beta1-integrins. *Exp. Cell Res.* **265**, 135-144.
- Ornitz, D. M. and Marie, P. J. (2002). FGF signaling pathways in endochondral and intramembranous bone development and human genetic disease. *Genes Dev.* **16**, 1446-1465.
- Patwari, P., Gaschen, V., James, I. E., Berger, E., Blakes, S. M., Lark, M. W., Grodzinsky, A. J. and Hunziker, E. B. (2004). Ultrastructural quantification of cell death after injurious compression of bovine calf articular cartilage. *Osteoarthr. Cartilage* **12**, 245-252.
- Velling, T., Risteli, J., Wennerberg, K., Mosher, D. F. and Johansson, S. (2002). Polymerization of Type I and III Collagens Is Dependent On Fibronectin and Enhanced By Integrins  $\alpha 11\beta 1$  and  $\alpha 2\beta 1$ . *J. Biol. Chem.* **277**, 37377-37381.
- Wennerberg, K., Lohikangas, L., Gullberg, D., Pfaff, M., Johansson, S. and Fässler, R. (1996). Beta 1 integrin-dependent and -independent polymerization of fibronectin. *J. Cell Biol.* **132**, 227-238.